

Intermetallic compound formed by electrodeposition of indium on antimony

Valentin M. Kozlov¹, Valeria Agrigento, Danilo Bontempi, Stefano Canegallo, Cleanthi Moraitou²,
Aikaterini Toussimi³, Luisa Peraldo Bicelli*, Giovanni Serravalle

Dipartimento di Chimica Fisica Applicata del Politecnico, Centro di Studio sui Processi Elettrodici del CNR, Via Mancinelli, 7, 20131 Milano, Italy

Received 2 December 1996; received in revised form 6 February 1997; accepted 6 February 1997

Abstract

Indium galvanostatic electrodeposition from aqueous solutions on antimony electrodes has been investigated together with time evolution of the deposit composition. The morphology, composition and structure of the deposit surface and cross-section have been analysed by SEM-EDS and X-ray diffraction both before and after annealing at 70, 110 and 135 °C for increasing times. The results showed the formation of InSb, owing to indium diffusion into the bulk of the cathode and to the reaction with antimony. The indium diffusion coefficient in InSb between 25 and 135 °C (from 0.1×10^{-19} to $2.6 \times 10^{-19} \text{ m}^2 \text{ s}^{-1}$) has been estimated from X-ray data and the values of the activation energy (30 kJ mol^{-1}) and preexponential factor ($1.8 \times 10^{-15} \text{ m}^2 \text{ s}^{-1}$) have been determined. © 1997 Elsevier Science S.A.

Keywords: Electrodeposition; Indium; Antimony; Intermetallic compound; Diffusion coefficient

1. Introduction

Compounds of the III–IV semiconductor family are widely used in many fields and the electrochemical synthesis of some of them has been subject of a number of publications. In previous papers [1–3], we investigated thin films of InBi prepared by In electrodeposition on Bi cathodes as well as the diffusion and reaction mechanism of formation of the other In–Bi intermetallic compounds (In_2Bi and In_3Bi_4). A very high average diffusion coefficient of In in InBi was found even at room temperature (around $10^{-15} \text{ m}^2 \text{ s}^{-1}$). The aim of this paper is to extend the research to InSb formation. This III–V compound is a low energy gap semiconductor (0.165 eV [4]) useful as material for IR detectors.

Several authors have investigated the codeposition of In

and Sb alloys from aqueous and non-aqueous baths and Sadana et al. [5] surveyed the literature data up to the end of 1983 also reporting the composition of the electrolytic baths (mainly containing In as InCl_2) and the plating conditions. Subsequently, Sadana and Singh [6] investigated aqueous solutions containing citrate complexes of the two metals to bring the deposition potentials closer. Indeed, the standard electrode potentials of the HSbO_3/Sb (pH above 1), SbO^+/Sb (pH below 1) and In^{3+}/In redox systems are 0.230, 0.212 and -0.342 V vs. NHE, respectively [7]. So, the potential difference between the Sb and In electrode, either 0.572 or 0.554 V, is rather large to permit a satisfactory codeposition from acidic solutions of the simple salts. X-ray analysis of the electrodeposited alloys showed that, according to the phase diagram [8], one intermediate phase, only, that is InSb, is present in this binary system.

Electrodeposition of InSb in an unstirred bath was shown to be a diffusion-controlled process in which the In/Sb concentration ratio has a great influence on the composition of the electrodeposited thin film [5,9]. In addition, Ortega and Herrero [10] showed the dependence of such composition on the electrodeposition potential and obtained polycrystalline InSb, free of In and Sb, from a bath containing citric acid and In and Sb chloride with an efficiency higher than 85%, at -0.318 V vs. In.

*Corresponding author

¹On leave from: Department of Physics, State Metallurgical Academy of Ukraine, Dnepropetrovsk, Ukraine.

²Present address: Department of Chemical Engineering, Section (III): Material Science, National Technical University, 9 Iroon Polytechniou Road, Zografou 157 73, Athens, Greece.

³Present address: Department of Chemical Engineering, Section (III): Material Science, National Technical University, 9 Iroon Polytechniou Road, Zografou 157 73, Athens, Greece.

A different method of preparing InSb thin films was proposed by Mengoli et al. [11] involving a sequential deposition from chloride baths, Sb first, then In. In was deposited at -0.268 V vs. In from a bath containing 0.3 M InCl_3 and 1 M KCl whose pH was adjusted to 1.5 – 2.0 with HCl . The two-layer samples, consisting of an inner Sb and an outer In layer (about 1 μm each) deposited on a Pt substrate, were then annealed at 150 , 175 and 185 $^\circ\text{C}$ for times from 1 to 15 h. Their percent conversion to InSb was determined as a function of time by stripping voltammetry in a strongly acidic solution (1.7 M HCl , 1.6 M H_2SO_4) and the results were qualitatively confirmed by X-ray diffraction (XRD). Only the In and Sb peaks were detected after annealing at 150 $^\circ\text{C}$, a temperature close to the In melting point (150.6 $^\circ\text{C}$) while both the typical peaks of InSb and of the unreacted components were present at 175 $^\circ\text{C}$, their relative amount depending on the annealing time. The single components peaks completely disappeared by annealing at temperatures equal to or higher than 185 $^\circ\text{C}$ for 5 – 10 h.

Hobson Jr. et al. [12] showed that the rate of formation of InSb at the interface between In and Sb at 100 $^\circ\text{C}$ is greatly increased when a composite electrode of In electrodeposited on Sb is made the cathode in an electrolytic cell. Indeed, the diffusion coefficient was lower than 2×10^{-18} $\text{m}^2 \text{s}^{-1}$ during the thermal synthesis of InSb and 1.5×10^{-16} $\text{m}^2 \text{s}^{-1}$ during the electrochemical synthesis. They maintained that the data available at the time of writing the paper were insufficient to explain such great difference in the diffusion rate.

Indium and Sb self-diffusion in InSb was investigated at 478 to 521 $^\circ\text{C}$ using a tracer technique and the activation energy and frequency factor were determined [13]. The data yielded different diffusion coefficients for group III and group V atoms in the compound 8.3 and 5.9×10^{-19} $\text{m}^2 \text{s}^{-1}$, respectively, at 478 $^\circ\text{C}$. InSb has the structure of the zinc-blende type with strong tetrahedral In–Sb coordination. If the two types of atoms were the same, the structure would be like that of Ge and Si. The diffusion coefficients in InSb are of the order of those for the substitutional elements in Ge thus tending to support a vacancy mechanism in this compound, too. A reasonable mechanism for self-diffusion accounting for above data seems to be vacancy diffusion in each of the face-centred cubic sublattices formed by the two constituents of InSb. On the basis of bond strength considerations, the authors could also assume that the diffusing entities in InSb are neutral atoms and explain the higher diffusion coefficient of In with respect to Sb.

2. Experimental

The Sb electrode, a cylinder of 16 -mm diameter, was prepared by melting Fluka Sb of 99.9% purity and its working surface was polished with silicon carbide paper.

The anode (counterelectrode) and the reference electrode (a thin foil inserted in a Luggin glass capillary) were of In (99.999% Fluka). The electrolyte was an aqueous solution 0.67 N of InCl_3 adjusted to pH 1.3 with HCl . The vertical Teflon electrochemical cell was used with the Sb working electrode on the bottom. All the measurements were performed in galvanostatic conditions ($555/\text{B}$ Amel potentiostat–galvanostat) and the cell voltage was measured with a $668/\text{RM}$ Amel potentiostat and recorded on paper (868 Amel). The potential of the Sb electrode vs. In was measured during and after electrodeposition with a 755 Yokogawa digital multimeter and stored on a magnetic medium allowing numerical postprocessing of the data by a personal computer. Seven runs were carried out at room temperature at current densities from 2 – 20 A m^{-2} obtaining In deposits from 0.026 – 0.164 - μm thick. These are the theoretical values assuming a uniform distribution (which was not the case, see below) and 100% In efficiency during electrodeposition as the selected experimental conditions were such that no parasitic hydrogen evolution took place. Time evolution of these very thin deposits was examined by monitoring the electrode potential after opening the circuit. Another set of deposits was prepared essentially in two different experimental conditions: thin In deposits (0.8 μm) at 10 A m^{-2} and thick (18 μm) ones at 5 A m^{-2} , in order to prove the formation of the intermetallic compound and to study the influence of temperature. At the end of the deposition process, the electrodes were immediately removed from the electrolyte to avoid In dissolution into the bath, rinsed in water, dried and annealed at 70 $^\circ\text{C}$ in an air thermostat and at 110 and 135 $^\circ\text{C}$ in an air oven for increasing times (up to several hundreds of hours). The deposit surface and cross-section (the samples were cut after immersion in liquid nitrogen for a few seconds) were submitted to SEM and EDS (Stereoscan 360, Cambridge Instrument and AN10/25-Link) and to XRD (PW7010, Phillips, $\text{Cu K}\alpha$). All the measurements were repeated several times and the average value of each run was considered.

3. Results and discussion

3.1. SEM and XRD results

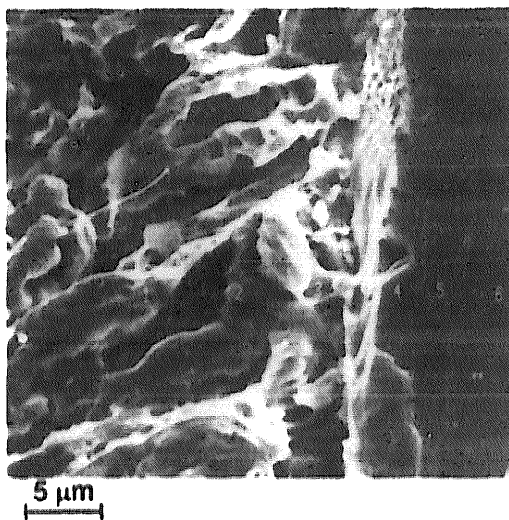
Thin (0.8 μm) In deposits obtained at room temperature were discontinuous and consisted of isolated microcrystals having an average size of 5 μm and showing quite regular crystal planes. The morphology did not substantially change in the examined time range. EDS evidenced these crystals being due to In whereas on the remaining regions of the surface only Sb was found. By heating the deposits, the surface of the microcrystals became rounded. This was more especially evident at the highest temperature (135 $^\circ\text{C}$) not far from the In melting point.

Thick (18 μm) deposits were rough and imperfect with typical holes but the In dot map analysis of their cross-section showed their practical continuity. SEM-EDS was performed at several points of this section from the surface towards the bulk of the specimen. An example is shown in Fig. 1(a) for a deposit observed two years after electrodeposition. The analysed points are labelled with progressive numbers. They show (Fig. 1(b)) the continuous decrease in the In atomic percentage which reaches a value close to 50% at the deposit–substrate interface, thus indicating the formation of InSb. At higher temperatures, the deposits were continuous (Fig. 1(c) shows a topographic view) and it was easier to observe InSb, for example after heating the deposit for 334 h at 110 $^{\circ}\text{C}$ (Fig. 1(d) shows the sample cross-section). This sample was scanned as to In composition along the white line in the micrograph

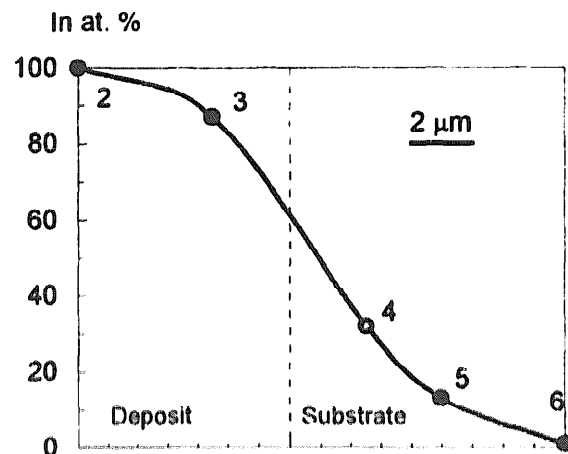
and the In-line profile was reported below the SEM image. Although such a profile was difficult to read because of the skewness of the surface, the comparison of the ratio between the height of the peaks with that between the theoretical In/Sb concentration showed that the sample had the three-layer structure In/InSb/Sb from the surface to the bulk.

The XRD pattern of the thicker deposits practically showed only the In peaks. Indeed, X-rays were completely absorbed in the external part of the deposit and could not reach the In/InSb interface, the intermetallic compound lying beyond their penetration depth.

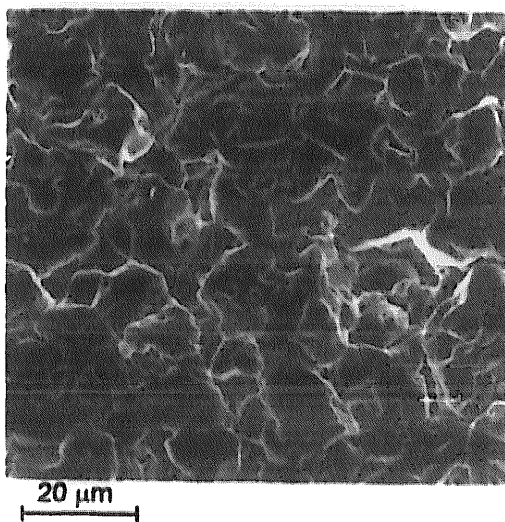
Fig. 2 compares the schematic ASTM peaks of In, Sb and InSb [14] with the XRD pattern of a thin (0.8 μm) deposit heated at 135 $^{\circ}\text{C}$ for 51.5 h. Although some lines are superimposed in the ASTM spectra, it was possible to



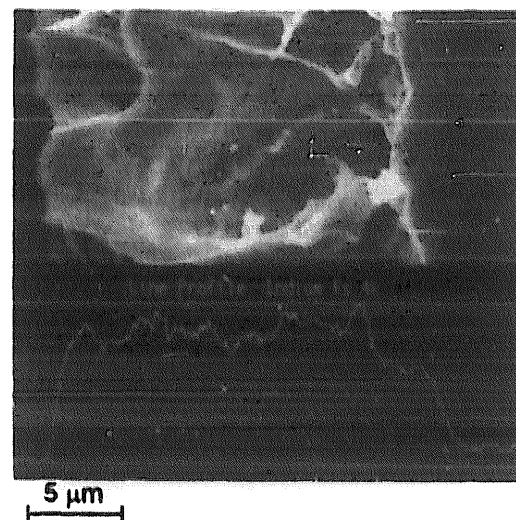
(a)



(b)



(c)



(d)

Fig. 1. SEM images of the cross-section (a) and (d) and of the surface (c) of 18- μm thick In electrodeposits. (a) deposit observed two years after electrodeposition; (b) Indium atomic percentage in several points of the sample (a); (c) and (d) deposits heated at 110 $^{\circ}\text{C}$ for 189 and 334 h, respectively; (d) the In-line profile (scanned along the white line in the micrograph) is reported in the lower part of the picture.

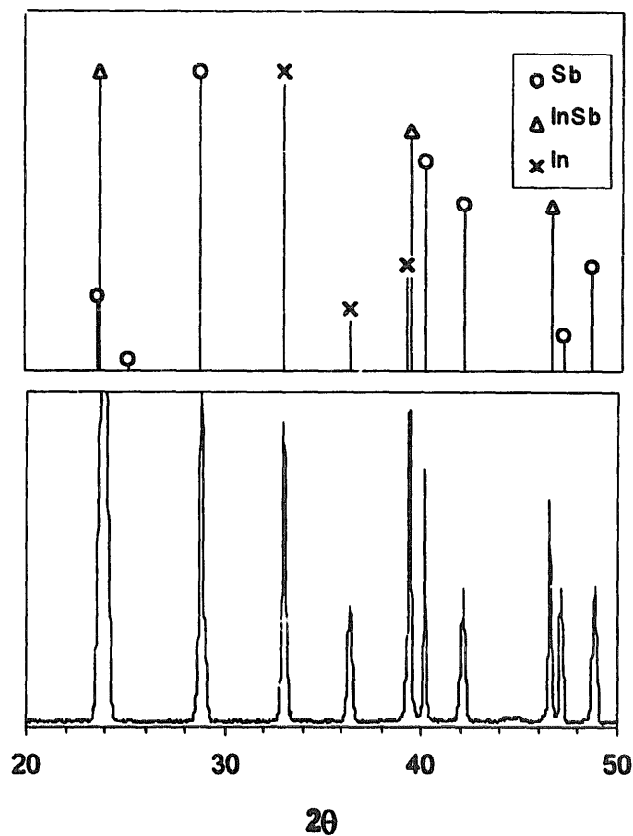


Fig. 2. Comparison of the schematic ASTM lines of In, Sb and InSb [14] with the XRD pattern of a 0.8- μm thick deposit heated at 135 °C for 51.5 h.

select for each phase at least one typical reflection peak not influenced by the nearby ones. This peak is at $2\theta = 28.6^\circ$ for Sb, and is due to the {012} plane, at 33.0° for In ({101}) and at 46.6° for InSb ({311}). The comparison of the sample peaks with the ASTM identification peaks shows that the deposit contained In and InSb.

In conclusion, EDS and XRD results undoubtedly showed the increasing formation of the InSb phase both with time and temperature. However, owing to the very low rate of the solid-state diffusion and reaction process, InSb could be detected either after aging the deposit for a very long time at room temperature or after a severe annealing.

3.2. Indium diffusion coefficient

To estimate the In diffusion coefficient in InSb at different temperatures, we considered the time decrease of the most intense In line ({101}) in the XRD pattern of the thin In deposits (0.8 μm). Always examining the same sample area, we assumed that the intensity of this line is proportional to the In moles in the deposit. So, if m_{dep} and m_{rem} are the In moles deposited on and removed by diffusion from the unit surface area, respectively, we have

$$m_{\text{rem}} = m_{\text{dep}} \left(1 - \frac{I_1}{I_0} \right) \quad (1)$$

where I_0 and I_1 are the intensities of the In line immediately after deposition and after heating the deposit, respectively. As expected (Fig. 3), the I_1/I_0 ratio decreased with the heating temperature.

According to Faraday's law:

$$m_{\text{dep}} = \frac{it_{\text{dep}}}{zF} \quad (2)$$

i being the current density, t_{dep} the time of deposition, F the Faraday's constant and $z=3$. Moreover, according to Schmalzried [15], assuming In diffusion, we have:

$$m_{\text{rem}} = \sqrt{D^*t_1} \quad (3)$$

where t_1 is the diffusion time (here the heating time) and D^* is proportional to the In diffusion coefficient, D . A square root-time dependence is assumed since the sample surface was covered with In after electrodeposition and, therefore, the growth rate of the InSb layer in between the In deposit and the Sb substrate was controlled by the solid-state diffusion and reaction process. The Schmalzried's theory, discussed in detail for the similar case of InBi formation (see [2]), implies that local thermodynamic equilibrium is maintained within the reaction layer and at the phase boundaries and that the In activity within the region of homogeneity of the InSb phase does not vary by more than a power of ten, so that an average D value over the reaction layer may be considered. This simplification is applicable to intermetallic compounds with a standard Gibbs free energy of formation from the elements, ΔG° , higher than -100 kJ mol^{-1} , as in our case ($-25.5 \text{ kJ mol}^{-1}$ [16]).

During these considerations, we assumed that only In diffused into InSb. As a matter of fact, In diffusion is

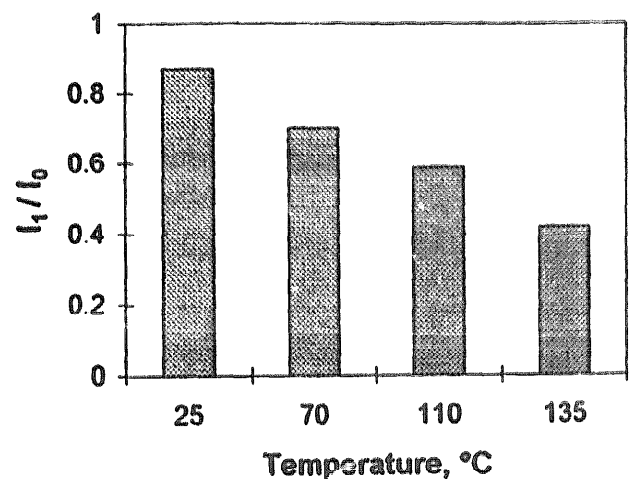


Fig. 3. Influence of the heating temperature of 0.8- μm thick In deposits on the relative intensity of the In {101} XRD line. Heating time: 100 h.

expected to prevail over that of Sb, owing to the higher mobility of In, as shown by the much lower melting point: 150.61 and 630.71 °C for In and Sb, respectively. Note that in the case of both In and Sb diffusion, the obtained diffusion coefficient would represent the sum of the two individual coefficients.

The diffusion coefficient depends on D^* [2] according to:

$$D = -\left(\frac{M}{\rho}\right)^2 \frac{RT}{2\Delta G_i^\circ} D^* \quad (4)$$

where R , T , M and ρ represent gas constant, temperature (298 K), InSb molecular weight (236.57 g mol⁻¹) and mass density (5.777 g cm⁻³), respectively.

So, introducing Eq. (4) in Eq. (3), results in:

$$m_{\text{rem}} = \frac{\rho}{M} \sqrt{-\left(\frac{2D\Delta G_i^\circ t_i}{RT}\right)} \quad (5)$$

and equating Eq. (1) to Eq. (5), taking Eq. (2) into account, we finally obtain the dependence of the diffusion coefficient from the I_1/I_0 ratio. Table 1 reports the D values and their standard deviation evaluated assuming no Sb diffusion and utilising the standard value at 25 °C for the Gibbs free energy.

From the linear dependence of $\ln D$ on $1/T$, we determined the activation energy (30 ± 2 kJ mol⁻¹) and the frequency factor ($1.8 \pm 0.5 \times 10^{-15}$ m² s⁻¹) of the diffusion process.

The results prove that In diffusion into and reaction with Sb to form the new InSb phase is a very slow process at room temperature. The value of the average diffusion coefficient ($\sim 10^{-20}$ m² s⁻¹) may well be compared with those for common metals and semiconductors (Ge and Si) which are in the range 10^{-20} – 10^{-30} m² s⁻¹ [17].

As stated in Section 1, Mengoli et al. [11] determined the time dependence of the percent conversion to InSb of In–Sb samples at high temperatures. As the initial quantities of In and Sb were known, we evaluated from these data the InSb moles formed on the unit surface area as a function of time. A square root dependence was found which allowed estimation of the diffusion coefficient. The D values turned out to be $\sim 3 \times 10^{-18}$ and 7×10^{-18} m² s⁻¹, at 175 and 185 °C, respectively, in agreement with our results, considering that at these temperatures In was in the molten state.

Our D value is about one order of magnitude lower than that obtained by Hobson Jr. et al. [12] during the thermal

synthesis of InSb at 100 °C. So far, their very high value obtained during the electrochemical synthesis remains unexplainable and perhaps not convincing. Indeed, by applying Schmalzried's relationship [15] to their data, we found an even higher diffusion coefficient (10^{-12} instead of 10^{-16} m² s⁻¹).

3.3. Structural and physicochemical aspects

Contrary to what was observed in the case of In electrodeposition on Bi cathodes, the In diffusion coefficient in InSb is very low, about five orders of magnitude lower than that in InBi where D is $\sim 10^{-15}$ m² s⁻¹ at room temperature [3]. This difference may be related to the different structures.

Most of the 1:1 compounds formed by elements of groups IIIA and VA of the periodic table to which In, and Sb and Bi belong (e.g., AlP, AlSb; GaP, GaAs, GaSb; InP, InAs, InSb) crystallize with the zinc-blende (cubic) structure with tetrahedrally coordinated atoms and strong covalent bonds (Fig. 4(a), [18]). The distance of the closest approach of In and Sb in InSb is for example 2.80 Å. Exceptions in this series are the compounds involving the more metallic elements, such as TlSb and TlBi, in which the atoms are in the cesium–chloride (cubic) arrangement and the interatomic distances are equivalent to the sum of the metallic radii for eightfold coordination (Fig. 4(b), [18]). InBi is intermediate between these two structural types as it has a tetragonal unit cell and metallic bonds with four-fold coordination. The B-10 structural type (Fig. 4(c), [18]) to which InBi belongs consists of layers of like atoms normal to the c axis with adjacent In layers separated by two Bi layers (AB₁B₂A stacking). Each In layer is bonded to the Bi layer of either side of it and the closest In–Bi interatomic distance (3.13 Å) is appreciably greater than the value expected for a covalent bond (2.92 Å) or for an ionic structure (2.86 Å) and even also much greater than the interatomic distance for the covalent bond in InSb (2.80 Å). Moreover, the closest approach of Bi atoms in neighbouring Bi layers is 3.68 Å, which is somewhat larger than the interatomic separation of Bi atoms in adjacent layers of metallic Bi (3.47 Å). This arrangement gives rise to a marked cleavage plane normal to the c axis [19]. A structure of this type can also be described as a distorted cesium–chloride arrangement when the axial ratio c/a approaches the value of $\sqrt{2}/2$ (0.707) and the distance between the layer A and the layers B₁ and B₂ approximates 0.5 c so that the atoms in the layers B₁ and B₂ lie now in the same plane (ABA stacking). However, in this case, the distortion is so great that a four-fold coordination results and only a formal resemblance exists between InBi and a distorted cesium–chloride arrangement.

The structure of InBi with typical layers is expected to be highly favourable to diffusion, particularly in the case

Table 1
Indium diffusion coefficient in InSb as a function of temperature

Temperature (°C)	25	70	110	135
$D \times 10^{19}$ (m ² s ⁻¹)	0.10 ± 0.04	0.58 ± 0.08	1.22 ± 0.10	2.59 ± 0.33

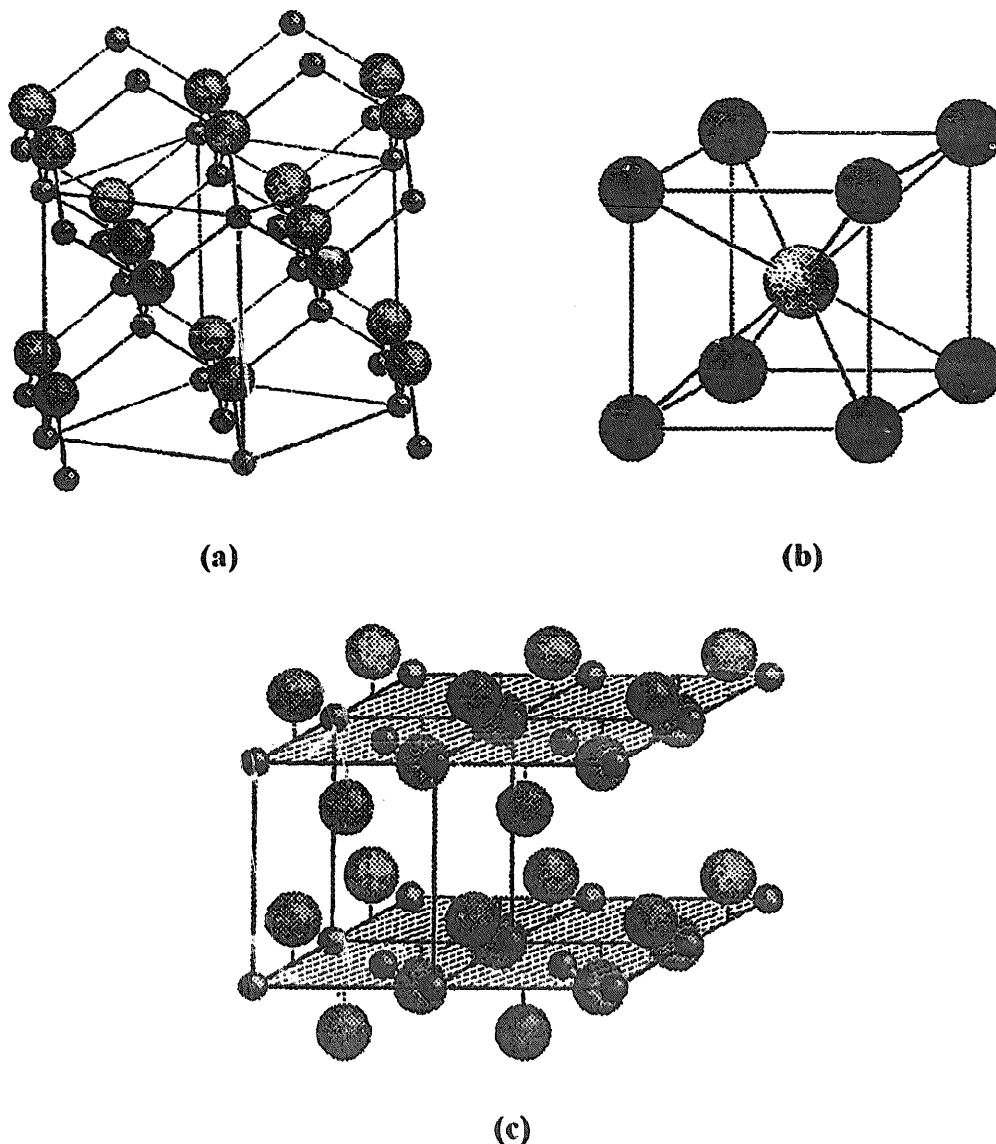


Fig. 4. Atomic arrangement in (a) zinc blende (B-3 structural type), (b) cesium chloride (B-2) and (c) lithium hydroxide (B-10) (from [18]). Four unit cells are shown in the latter case to evidence the layered structure.

of metals, such as In, which has a low melting point and, thus, a high mobility. On the contrary, a compound such as InSb, with strong bonds and a more compact atomic arrangement, is expected to be more 'impervious'.

It is now worth recalling that in our case the In diffusion process is accompanied by a chemical reaction to form the intermetallic compound. As shown in Eq. (3), the In quantity removed from the unit surface area of the deposit in the time unit depends on D^* which, according to Eq. (4), is proportional not only to the diffusion coefficient but also to the Gibbs free energy of formation from the elements of the intermetallic compound: $-25.5 \text{ kJ mol}^{-1}$ for InSb [16] and -3.7 kJ mol^{-1} for InBi [20], in standard conditions. Indeed, this thermodynamic quantity represents the difference between the In chemical potential at the two phase boundaries of the reaction product. As shown, its absolute value is much higher in InSb than in InBi but not

high enough to compensate for the difference in the diffusion coefficients. Consequently, since the constant in Eq. (4) is nearly the same for the two compounds, m_{rem} in the time unit is much lower for InSb than for InBi and it was not possible to observe the deposited In microcrystals collapse on and disappear from the sample surface as occurred in the case of In deposits on Bi cathodes [1]. So, the structural factors prevail over the physicochemical ones.

4. Conclusions

Indium electrodeposition on Sb cathodes showed the formation of the InSb intermetallic compound. Moreover, XRD data showed that the In diffusion coefficient in this phase could be determined from the intensity of the

strongest In line as a function of time after In deposition and of the annealing temperature.

In general, diffusion and reaction processes in the solid state are scarcely reproducible phenomena owing to the consistent influence of the crystal geometry (surface coverage, material morphology) and structure (single crystals or polycrystals, preferred orientation, grain size, dislocation density and other lattice defects) so that only the order of magnitude of the average diffusion coefficient is significant. Since the geometry and structure of both the In deposit and the Sb substrate depend on the way they were prepared, the values we obtained for the In diffusion coefficient (e.g. $D=10^{-20} \text{ m}^2 \text{ s}^{-1}$ at 25 °C) refer to In electrodeposits on a bulk Sb substrate. A more detailed investigation on these aspects may be illuminating. Moreover, the structural and physicochemical considerations have shown the interest in investigating the formation of other 1 to 1, III–V compounds and suggest promising research in this area, too.

Acknowledgments

C. Moraitou and A. Toussimi are indebted to the Time (Erasmus) program for a grant. The research was carried out with the financial support of the Ministero della Università e della Ricerca Scientifica e Tecnologica.

References

[1] S. Canegallo, V. Demeneopoulos, L. Peraldo Bicelli, G. Serravalle, J. Alloys Comp. 216 (1994) 149.

- [2] S. Canegallo, V. Demeneopoulos, L. Peraldo Bicelli, G. Serravalle, J. Alloys Comp. 228 (1995) 23.
- [3] S. Canegallo, V. Agrigenio, C. Moraitou, A. Toussimi, L. Peraldo Bicelli, G. Serravalle, J. Alloys Comp. 234 (1996) 211.
- [4] J.C. Wooley, J. Warner, Can. J. Phys. 42 (1964) 1879.
- [5] Y.N. Sadana, J.P. Singh, R. Kumar, Surf. Technol. 24 (1985) 319.
- [6] Y.N. Sadana, J.P. Singh, Plat. Surf. Fin. 64 (1985) 64.
- [7] M. Pourbaix, Atlas of Electrochemical Equilibria in Aqueous Solutions, 2nd ed.; NACE, Houston, TX, and CEBELCOR, Brussels, 1974, p. 436 (In), 524 (Sb).
- [8] T.B. Massalski, Binary Alloy Phase Diagrams, Vol.2, American Society of Metals, Ohio, 1986, p. 1395.
- [9] T. Okubo, M. Landau, Abstract 376, The Electrochemical Society Extended Abstracts, Vol. 88-2, Chicago, IL, Oct. 9–14, 1988, p. 547.
- [10] J. Ortega, J. Herrero, J. Electrochem. Soc. 136 (1989) 3388.
- [11] G. Mengoli, M.M. Musiani, F. Paolucci, M. Gazzano, J. Appl. Electrochem. 21 (1991) 863.
- [12] M.C. Hobson Jr., H. Leidheiser Jr., Trans. Met. Soc. AIME 233 (1965) 482.
- [13] F.H. Eisen, C. Birchenall, Acta Met. 5 (1957) 265.
- [14] ASTM Cards: 5-0642, 1974 (In); 35-732, 1990 (Sb); 6-0298, 1967 (InSb).
- [15] H. Schmalzried, Solid State Reactions, Academic Press, New York, 1974, pp. 53–66; 95–97; 124–127.
- [16] D.D. Wagman, V.H. Evans, V.B. Parker, R.H. Schumm, I. Halow, S.M. Bailey, K.L. Churney, R.L. Nuttall, J. Phys. Chem. Ref. Data 11, Suppl. 2 (1982) 2–134.
- [17] C.A. Wert, R.M. Thomson, Physics of Solids, McGraw-Hill, New York, 1970, pp. 54–67.
- [18] Landolt-Boernstein, Zahlenwerte und Funktionen, Sechste Auflage, I Band, Atom- und Molekularphysik, 4. Teil, Kristalle, Springer-Verlag, Berlin, 1955, p. 24 (B-2 type); pp. 24–25 (B-3 type); p. 27 (B-10 type).
- [19] P. Binnie, Acta Cryst. 9 (1956) 686.
- [20] P.Y. Chevalier, Calphad 12 (1988) 383.